J Mater Sci: Mater Electron (2016) 27:8753–8757
DOI 10.1007/s10854-016-4898-2

# Fabrication and improved photocatalytic activity of *n*-ZnO nanorod arrays/*p*-CuO thin film heterojunction

**Duo Li[1] · Shiyong Gao[1,2] · Jinzhong Wang[1] · Lin Li[2] · Qingjiang Yu[1] · Shujie Jiao[1] · Yong Zhang[1] · Dongbo Wang[1] · Fengyun Guo[1] · Liancheng Zhao[1]**

Received: 16 March 2016 / Accepted: 25 April 2016 / Published online: 5 May 2016


**Abstract** ZnO nanorod arrays (NRs) are successfully synthesized on CuO thin film by hydrothermal method. The result of scanning electron microscopy demonstrates that the ZnO NRs produce great changes on morphology after deposited on CuO thin film. The current–voltage measurement of ZnO NRs/CuO film heterostructures show an evident rectifying behavior. Furthermore, the photocatalytic activity is investigated by degradation of methyl orange dye. It is found that compared with ZnO NRs, ZnO NRs/CuO film heterostructures display a better photocatalytic activity.

## 1 Introduction

Since the environmental problems relating to organic and toxic waste in water endangered human health and inhibited economic development, photocatalysis as an efficient and environmental-friendly way to manage water pollution has received extensive attention in recent years [1, 2]. Nowadays semiconductor materials have been widely used in photocatalytic fields due to their outstanding catalytic activity [3, 4]. Among many semiconductor materials, ZnO becomes a very promising candidate for applications in photocatalysis because of its superior properties such as high photocatalytic activity, easy synthesis, low cost and non-toxicity [5]. However, the applications for photocatalysis of ZnO are also constrained by its two major drawbacks. One problem is that since it is a wide band gap (3.37 eV) semiconductor, ZnO can only be activated by UV light irradiation which occupies a small part of solar irradiance (3–5 %) [6]. The other issue is the high recombination rate of photogenerated electrons and holes. This reduces the quantum efficiency of ZnO and deteriorates its photocatalytic activity [7]. Therefore, how to extend its absorption spectrum and reduce the recombination rate of photogenerated carriers are very important in promoting photocatalytic activity of ZnO [8].

To solve these issues, people have conducted a lot of research including doping [9], metal composite [10], quantum dots sensitized [11] and heterostructure composite [12] in the past decades. Among these methods, to form heterostructures combined with other *p*-type semiconductors is an efficient way to enhance the photocatalytic ability. As a narrow band gap *p*-type semiconductor [13], CuO has been proved as an ideal candidate to compose with ZnO [14]. On one hand, CuO can form bandgap complementary with ZnO to extend absorption spectrum; on the other hand it can combine with ZnO to form heterojunctions which can efficiently hinder the recombination of photogenerated carriers. In addition, CuO has many other unique properties such as large interfacial areas, highly reactive surfaces, distinctive optical property and unusual catalytic property [15]. Liu et al. [16] have recently demonstrated the photocatalytic activity of mesoporous ZnO could be remarkably enhanced through coupling with CuO quantum dots. Concerning the core–shell CuO/ZnO nanoparticles were synthesized, Yang et al. [17] proved these composited structures display

✉ Shiyong Gao
gaoshiyong@hit.edu.cn

✉ Jinzhong Wang
jinzhong_wang@hit.edu.cn

[1] School of Materials Science and Engineering, Harbin Institute of Technology, Harbin 150001, China

[2] Key Laboratory for Photonic and Electric Bandgap Materials, Ministry of Education, Harbin Normal University, Harbin 150025, China

unbelievable photocatalytic activity. Shreyasi et al. [18] reported that the synthesized ZnO/CuO heterostructures at low temperature can present excellent photocatalytic properties under visible light irradiation. However, much less work has been devoted to preparing ZnO nanorod arrays (NRs) on CuO film for enhancing photocatalytic efficiency.

In this paper, ZnO NRs were carried out on CuO thin film through hydrothermal method. The microstructures and morphologies of ZnO NRs/CuO film heterostructures were characterized. The optical properties and photocatalysis mechanism of the ZnO NRs/CuO film heterostructures were investigated.

## 2 Experimental

### 2.1 Sample preparation

CuO thin film was deposited on ITO substrates (10 mm × 10 mm) using radio frequency (RF) magnetron sputtering system. When the base pressure reached $1 \times 10^{-3}$ Pa, argon gas (40 sccm) and oxygen gas (5 sccm) were led into vacuum chamber to form mixed atmosphere. The CuO film deposition was performed at the sputtering pressure of 1.0 Pa and the power of 100 W.

Then the ZnO seed layers were coated on CuO thin film using RF magnetron sputtering method. The prepared samples were annealed at a temperature of 400 °C for 0.5 h in air. After that, they were immersed into mixed aqueous solution containing 0.05 M zinc acetate dehydrate ($Zn(CH_3COOH)_2{\cdot}2H_2O$) and hexamethylenetetramine ($C_6H_{12}N_4$). Then the solution was transferred into the Teflon-lined stainless steel autoclave. The mixture was performed in a hot air oven at 95 °C for 6 h. After the oven cooled to room temperature, the samples were taken out followed by rinsing and drying. For the purpose of comparison, the ITO substrate without CuO film was also applied for the same hydrothermal process.

### 2.2 Sample characterization

The crystal structures of the prepared samples were identified by X-ray diffraction (XRD, Bruke D8 advance with Cu Ka radiation). The morphology was characterized by field-emission scanning electron microscopy (FE-SEM, Hitachi-SU70). The UV–Vis absorption spectra were recorded on a spectrophotometer (TU1901) and the current–voltage (*I–V*) measurements were performed by electrochemical workstation (CS350). The electrical properties of CuO film was obtained by the van der Pauw method at room temperature in a HALL8800 system.

### 2.3 Photocatalytic activity

To estimate the photocatalytic activity of the ZnO NRs/CuO film heterostructures, a methyl orange (MO) aqueous solution (10 mg/L) was chosen as the simulation of industrial pollutants. A xenon lamp (CEL-S500) was used as a light source. The samples were immersed into the MO solution (4 mL) which was put in the light irradiation. The variation of MO concentration with irradiation time was measured using a UV–Vis spectrophotometer (Phenix, UV1700PC). The degradation efficiency is reported as $C/C_0$, where C is the concentration of MO solution at the irradiation time t, $C_0$ is the initial concentration.

## 3 Results and discussions

The as-deposited CuO film showed *p*-type conduction with a hole concentration of $4.65 \times 10^{15}$ $cm^{-3}$ at room temperature. Figure 1 shows the XRD patterns of the as-prepared ZnO NRs and ZnO NRs/CuO film heterostructures. As for ZnO NRs, the characteristic peaks with 2θ value of 31.5°, 34.2°, 36°, 47.2° and 62.6° are corresponded to ZnO (100), (002), (101), (102) and (103) planes (JCPDS no. 36-1451). And two diffraction peaks located at 30.5° and 35.5° are attributed to ITO substrate. Notably, after fabricated on CuO film, an additional peak positioned at 35.2° emerged firstly, which can be assigned to CuO (002) plane (JCPDS no. 44-0706). Secondly, the preferential orientations of (002) and (004) crystal planes corresponding to ZnO NRs were observed and the narrow diffraction peaks revealed the ZnO NRs have high crystal quality. Finally, no position shift of ZnO (002) peak demonstrated CuO film did not change the intrinsic property of ZnO crystals.

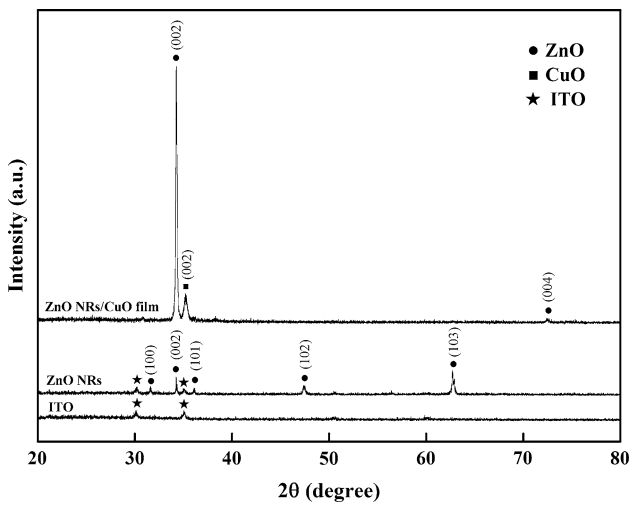


**Fig. 1** XRD patterns of ZnO NRs/CuO film heterostructures, ZnO NRs and ITO substrate

Figure 2a is the SEM image of ZnO NRs grown on ITO glass. All nanorods had smooth surfaces and planar top ends owing to their hexagonal structures and grew toward different directions with the diameters from 10 to 100 nm (the inset of Fig. 2a). The morphology of ZnO NRs/CuO film heterostructures is shown in Fig. 2b. It can be obviously seen that after fabricated on CuO thin film, the ZnO NRs became slim and uniform with the diameters almost about 30 nm. Moreover, every dozens of ZnO NRs were overlapped with each other and all tops of ZnO NRs were reunited into clusters forming like-tower structures (the inset of Fig. 2b). The reason for this change may result from the differences when seed layers were conformed. When deposited on CuO thin film, ZnO seed layer (Fig. 2d) generates more nucleation sites compared with that (Fig. 2c) deposited on ITO substrate within the same area, suggesting the size of ZnO nucleation becomes smaller or that it has larger nucleation density. Therefore after hydrothermal process, the ZnO NRs grown on CuO thin film will become more slim and uniform than that grown on ITO substrate.

The UV–Vis absorption spectra were examined to analyze the optical properties of ZnO NRs and ZnO NRs/CuO film heterostructures (Fig. 3a). Definitely the absorption edge of the ZnO NRs appears at ~380 nm and almost has no absorption in visible light region due to its large energy gap. However the spectrum of the ZnO NRs/CuO film heterostructures apparently shows a red shift into visible light region at ~500 nm. This demonstrated CuO thin film played an important role to overlap energy band of ZnO NRs, indicating the absorption spectrum of ZnO NRs extends to visible light region when combined with CuO thin film [14, 19].

Figure 3b shows the *I–V* characteristic of ZnO NRs/CuO film heterojunctions measured at room temperature. A schematic diagram of the *n*-ZnO NRs/*p*-CuO film heterojunction diode is presented in the inset of Fig. 3b, where a bias voltage was applied across Indium electrons coated on ZnO NRs and CuO film. It was found that the output current clearly exhibits the typical diode rectifying characteristic and the rectification ratio is 54 at 3 V.

The MO degradation of ZnO NRs and ZnO NRs/CuO film heterostructures are exhibited in Fig. 4a. The direct photolysis of MO without catalyst was not observed, which indicated the self-photolysis was negligible. The ZnO NRs had the photocatalytic degradation rate of 30 % after 1 h. As expected, ZnO NRs/CuO film heterostructures exhibited higher photocatalytic activity than ZnO NRs under the same experimental conditions. Figure 4b shows the recyclability test of photocatalytic decomposition for ZnO NRs/CuO film heterostructures. After five cycles of photocatalytic degradation, no significant loss of activity was observed, which indicated that these composed structures had good stability and reusability.

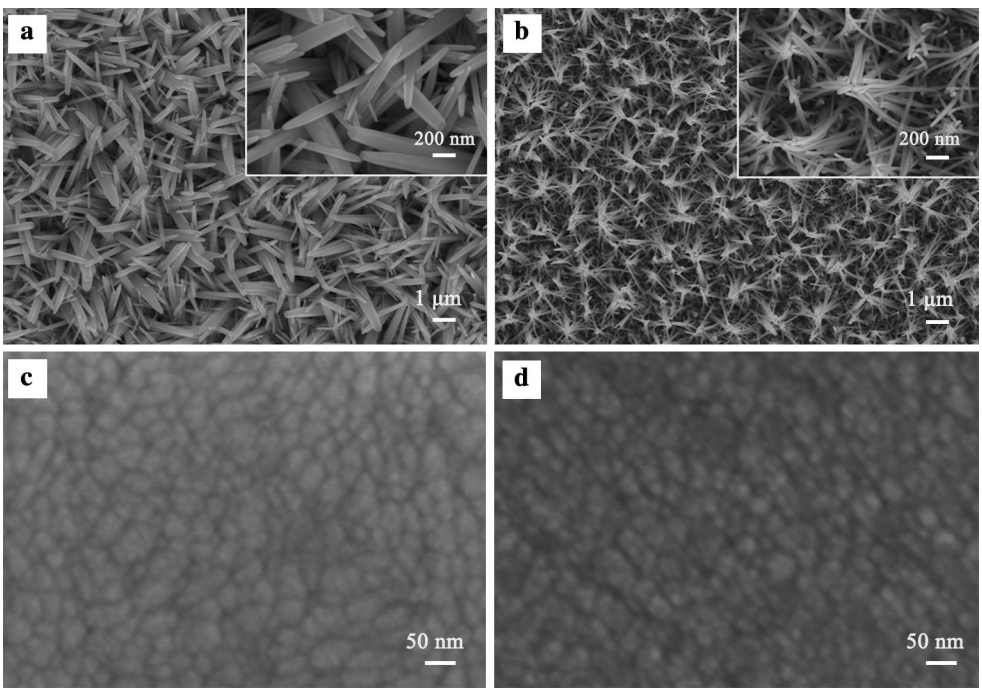


**Fig. 2** SEM images of **a** ZnO NRs and **b** ZnO NRs/CuO film heterostructures. The *insets* of (**a**) and (**b**) are high magnifications, **c** and **d** are the SEM images of ZnO seed layer grown on ITO substrate and CuO thin film

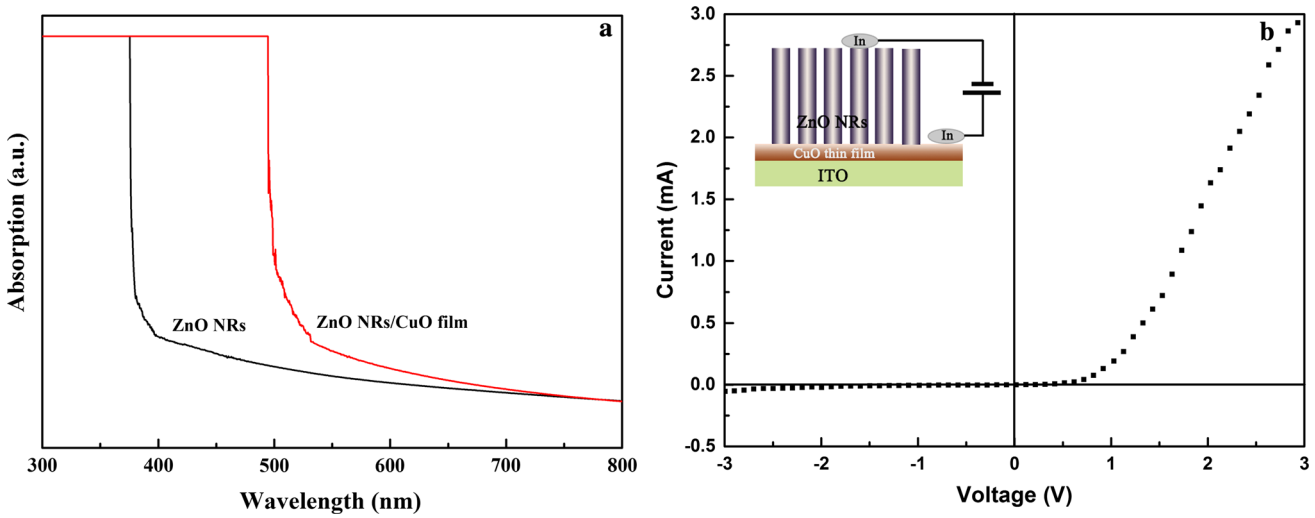


**Fig. 3** **a** The UV–Vis absorption spectra of the ZnO NRs and the ZnO NRs/CuO film heterostructures, **b** *I–V* characteristic of *n*-ZnO NRs/*p*-CuO film heterojunctions at room temperature, the *inset* is the schematic diagram of the *n*-ZnO NRs/*p*-CuO film heterostructures

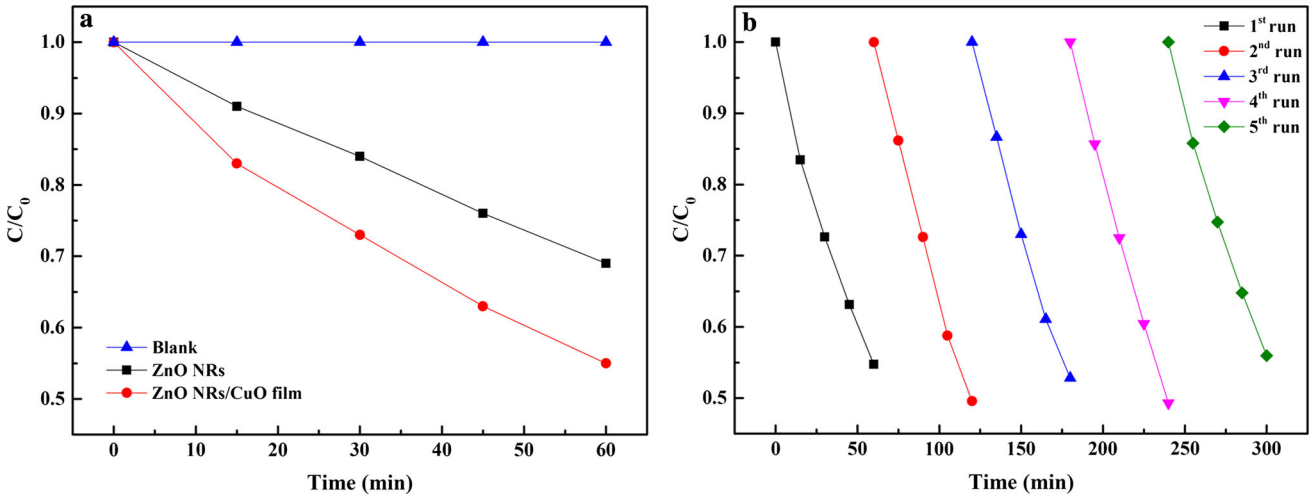


**Fig. 4** **a** Photodegradation rate of MO by ZnO NRs and ZnO NRs/CuO film heterostructures, **b** recyclability test of photocatalytic decomposition for ZnO NRs/CuO film heterostructures

Based on the experimental results, the mechanism of the photocatalytic activity of the ZnO NRs/CuO film heterostructures has been proposed as shown in Fig. 5. When ZnO and CuO form a heterojunction, the electrons transfer from *n*-type ZnO to *p*-type CuO while the holes transfer from CuO to ZnO until the system gets a uniform Fermi level. Then, an internal electric field is created at the interface between CuO and ZnO. Consequently, when the ZnO NRs/CuO film heterostructures are illuminated by light, electrons in the valence band (VB) of ZnO and CuO can be excited to their conduction band (CB), while the holes remain in VB. And then the photogenerated electrons transfer from the CB of CuO to that of ZnO under the effect of internal electric field. Analogously, photogenerated holes can move from the VB of ZnO to that of CuO [20]. Therefore the probability of the recombination of electron–hole pairs is significantly reduced resulting in the promotion of the photocatalytic activity. Moreover it is worth mentioning that since CuO can be reactivated by visible light irradiation due to its narrow band gap, the ZnO NRs/CuO film heterostructures synthesized extend the absorption range to visible light region. This is also consistent with the conclusion that is proved by UV–Vis absorption spectra. As a result, the photocatalytic efficiency of ZnO NRs/CuO film heterostructures can be enhanced significantly compared with that of ZnO NRs. The major reaction mechanism of photocatalytic decomposition by ZnO NRs/CuO film heterostructures can be described as follows: [21].

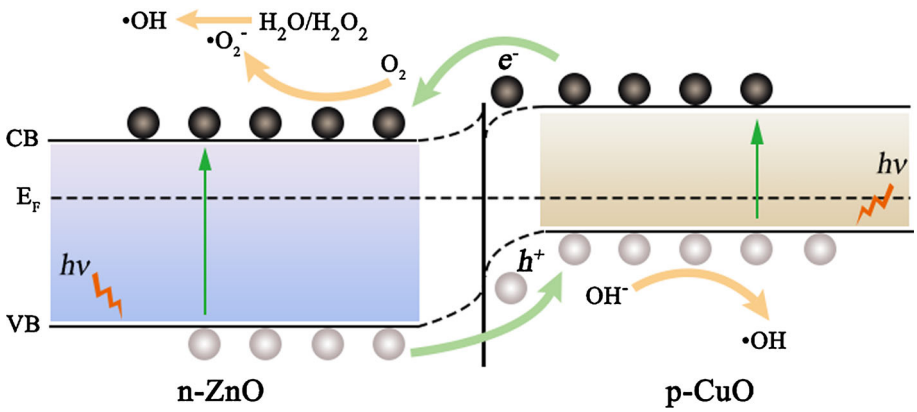


**Fig. 5** Schematic band diagram of *n*-ZnO/*p*-CuO heterojunctions at thermal equilibrium and the transfer processes of photogenerated carriers ($e^-$, electrons; $h^+$, holes); $E_F$, the Fermi energy; $E_g$, the energy gap; CB, conduction band; VB, valence band

$$\mathrm{ZnO/CuO} + h\nu \rightarrow \mathrm{CuO}\ (h^+)/\mathrm{ZnO}\ (e^-)$$
$$e^- + \mathrm{O_2} \rightarrow \cdot\mathrm{O_2^-}$$
$$h^+ + \mathrm{OH^-} \rightarrow \cdot\mathrm{OH}$$
$$\cdot\mathrm{O_2^-} + \mathrm{H_2O} \rightarrow \mathrm{H_2O_2} + \cdot\mathrm{OH}$$
$$\mathrm{H_2O_2} + \cdot\mathrm{O_2^-} \rightarrow \cdot\mathrm{OH} + \mathrm{OH^-} + \mathrm{O_2}$$
$$\mathrm{MO} + \cdot\mathrm{OH} \rightarrow \text{Degradation products}$$

## 4 Conclusions

In summary, ZnO NRs/CuO film heterostructures have been successfully synthesized on ITO substrate by a magnetron sputtering technique combined with hydrothermal method. The morphology of ZnO NRs produced great changes after fabricated on CuO film. The ZnO NRs/CuO film heterojunctions demonstrated good rectification characteristics and exhibited better photocatalytic performance than ZnO NRs. Furthermore, the superior stability and reusability were revealed by the recyclability test. The results demonstrated that ZnO NRs/CuO film heterostructures have a promising application for photocatalysis.

**Acknowledgments** The work was supported by National Science Foundation of China (Nos. 61306014 and 61574051), the Research Fund for the Doctoral Program of Higher Education of China (No. 20122302120009), the China Postdoctoral Science Foundation (No. 2013M540283), Heilongjiang Postdoctoral Foundation (LBH-Z11142), the Fundamental Research Funds for the Central Universities (No. HIT. NSRIF. 2014003), Natural Science Foundation of Heilongjiang Province of China (E2015002), and Open Project Program of Key Laboratory for Photonic and Electric Bandgap Materials, Ministry of Education, Harbin Normal University (PEBM201406).

## References

1. H. Tong, S.X. Ouyang, Y.P. Bi, N. Umezawa, M. Oshikiri, J.H. Ye, Adv. Mater. **24**, 229–251 (2012)
2. D. Chatterjee, S. Dasgupta, J. Photochem. Photobiol. C **6**, 186–205 (2005)
3. J.G. Lv, F.J. Shang, G.C. Pan, F. Wang, Z.T. Zhou, C.L. Liu, W.B. Gong, Z.F. Zi, X.S. Chen, G. He, M. Zhang, X.P. Song, Z.Q. Sun, F. Liu, J. Mater. Sci. Mater. Electron. **25**, 882–887 (2014)
4. V. Vaiano, O. Sacco, D. Sannino, P. Ciambelli, Appl. Catal. B **170–171**, 153–161 (2015)
5. S.S. Xiao, L. Liu, J.S. Lian, J. Mater. Sci. Mater. Electron. **25**, 5518–5523 (2014)
6. Y. Wang, G.W. She, H.T. Xu, Y.Y. Liu, L.X. Mu, W.S. Shi, Mater. Lett. **67**, 110–112 (2012)
7. H.G. Fan, X.T. Zhao, J.H. Yang, X.N. Shan, L.L. Yang, Y.J. Zhang, X.Y. Li, M. Gao, Catal. Commun. **29**, 29–34 (2012)
8. A.C. Dodd, A.J. McKinley, M. Saunders, T. Tsuzuki, J. Nanopart. Res. **8**, 43–51 (2006)
9. S. Anandan, A. Vinu, T. Mori, N. Gokulakrishnan, P. Srinivasu, V. Murugesan, K. Ariga, Catal. Commun. **8**, 1377–1382 (2007)
10. Y.S. Liu, S.H. Wei, W. Gao, J. Hazard. Mater. **287**, 59–68 (2015)
11. L.Y. Zhang, L.W. Yin, C.X. Wang, N. Lun, Y.X. Qi, ACS Appl. Mater. Interfaces **6**, 1769–1773 (2010)
12. S.Y. Gao, S.J. Jiao, B. Lei, H.T. Li, J.Z. Wang, Q.J. Yu, D.B. Wang, F.Y. Guo, L.C. Zhao, J. Mater. Sci. Mater. Electron. **26**, 1018–1022 (2015)
13. A.A. Al-Ghamdi, M.H. Khedr, M.S. Ansari, P.M.Z. Hasan, M.S. Abdel-wahab, A.A. Farghali, Phys. E **81**, 83–90 (2016)
14. P. Sathishkumar, R. Sweena, J.J. Wu, S. Anandan, Chem. Eng. J. **171**, 136–140 (2011)
15. Z.S. Hong, Y. Gao, J.F. Deng, Mater. Lett. **52**, 34–38 (2002)
16. Y.X. Liu, J.X. Shi, Q. Peng, Y.D. Li, Chem. Eur. J. **19**, 4319–4326 (2013)
17. C. Yang, X.D. Cao, S.J. Wang, L. Zhang, F. Xiao, X.T. Su, J.D. Wang, Ceram. Int. **41**, 1749–1756 (2015)
18. P. Shreyasi, M. Soumen, N.M. Uday, K.C. Kalyan, CrystEngComm **17**, 1464–1476 (2015)
19. S. Jung, K.J. Yong, Chem. Commun. **47**, 2643–2645 (2011)
20. K. Mageshwari, D. Nataraj, P. Tarasankar, R. Sathyamoorthy, P. Jinsub, J. Alloys Compd. **625**, 362–370 (2015)
21. R. Saravanan, S. Karthikeyan, V.K. Gupta, G. Sekaran, V. Narayanan, A. Stephen, Mater. Sci. Eng. C **33**, 91–98 (2013)